Crystal Structure of Poly(*tert*-Butylethylene sulfide): A Reappraisal in the Light of Frustration

Laurent Cartier,† Nicolas Spassky,‡ and Bernard Lotz*,†

Institut Charles Sadron (CNRS-ULP), 6, rue Boussingault, 67083 Strasbourg, France, and Université Pierre et Marie Curie, Laboratoire de Chimie Macromoléculaire 4, place Jussieu, 75232 Paris Cédex 05, France

Received December 22, 1997; Revised Manuscript Received February 24, 1998

ABSTRACT: The crystal structure of poly(*tert*-butylethylene sulfide) (PTBES) determined in 1977 by Matsubayashi et al. (*Macromolecules* **1977**, *10*, 996) is reexamined. Single crystals, of an unusual triangular shape, and epitaxially crystallized samples have been obtained and investigated by electron microscopy and electron diffraction. All the morphological and diffraction evidence indicates that PTBES has a "frustrated" crystal structure, i.e., a packing in which the azimuthal settings differ for the 3-fold helices. The crystal structure thus determined significantly improves that initially proposed for PTBES, within the trigonal crystal lattice determined by Matsubayashi *et al.* PTBES also illustrates the full range of experimental evidence that indicates the frustrated nature of the structure: characteristic diffraction patterns of single crystals and of epitaxially crystallized films (or of fibers) and triangular morphology of the single crystals.

Introduction

Poly(*tert*-butylethylene sulfide) (PTBES):

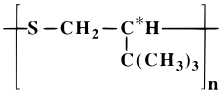

is one of several isotactic polymers with true asymmetric carbons in their main chains,[1] as opposed, for example, to isotactic polypropylene (iPP): as a result, it forms only helices of one hand, whereas iPP exists as both right- and left-handed helices. Both optically active and inactive PTBES are known: the latter is synthesized from racemic monomers using stereospecific initiator; the former is obtained from optically active monomer using anionic or stereospecific initiator.[2] The crystal structures of optically active and inactive polymers were determined in 1977 by Matsubayashi et al.[3] Both forms adopt a 3-fold helical structure with a fiber axis periodicity of 6.5 Å. The *racemate* crystallizes in a monoclinic unit cell in which (bi)layers of interdigitating right- and left-handed helices alternate along the *a* axis and therefore bears strong structural similarities with the monoclinic α structure of isotactic polypropylene (αiPP) and the trigonal unit cells of isotactic poly(1-butene) (iPBu1), form I, and isotactic polystyrene (iPS).

The crystal structure of the *optically active form* was shown to rest on a trigonal unit cell, with parameters $a = b = 16.91$ Å and $c = 6.50$ Å and space group $P3_1-C_3$,[2] which contains *three* right-handed 3_1 helices.[3] Difficulties were, however, encountered during the crystal structure derivation. In particular, it was noted that most reflections are accounted for on the basis of a smaller, trigonal unit cell with *one* chain; the three-chain cell develops only when the sample is annealed at 145 °C for 20 h. Also, the intensities of the weaker reflections characteristic of the larger cell could only be explained in terms of a statistical molecular packing with respect to upward and downward chains. More disturbingly, and at variance with common tenets of polymer crystallography, the conformation of the three side chains was supposed to be different: the torsional angle τ_4 connecting the *tert*-butyl to the main chain takes up three different values, which furthermore differ for up chains and for down chains.

In the present paper, we reexamine the crystal structure of the optically active form of PTBES, on the basis of the initial data and on new morphological and diffraction data obtained with the original sample.[3] This reinterpretation is based on the concept of frustrated polymer structures, i.e., on an original packing mode proposed recently for 3-fold isochiral helices.[4,5] The distinctive feature of this packing mode is the different azimuthal settings of the various helices, which leads "spontaneously" to a three-chain trigonal unit cell. The morphological analysis and structure derivation of PTBES actually provides a case example for the analysis of similar polymer structures and illustrates the potential of the concept of frustration in polymer crystallography.

Experimental Section

1. Samples. The sample of optically active PTBES is that used in the initial study of Matsubayashi et al.[3] It is prepared from (*S*)-*tert*-butylethylene sulfide and polymerized using diethylzinc−water (1/1) as a catalyst. The optical rotation for the polymer is $[\alpha]^{25}_D = 172$ ($CHCl_3$).

2. Sample Preparation. Single crystals of PTBES are produced most conveniently from thin films cast from toluene solutions (1−2% w/v) on cleaved mica sheets or glass cover slides. Thermal treatments are performed under a nitrogen atmosphere in a Mettler FP 80 heating stage controlled with a homemade program run on a PC. Melting at 180 °C is followed by a steep temperature decrease to the isothermal crystallization temperature, in the 120−150 °C range. Very large single crystals (by polymer standards) could be obtained under these conditions (cf. Figure 1a).

* To whom correspondence should be addressed.
† Institut Charles Sadron.
‡ Université Pierre et Marie Curie.

S0024-9297(97)01844-5 CCC: $15.00
Published on Web 04/21/1998

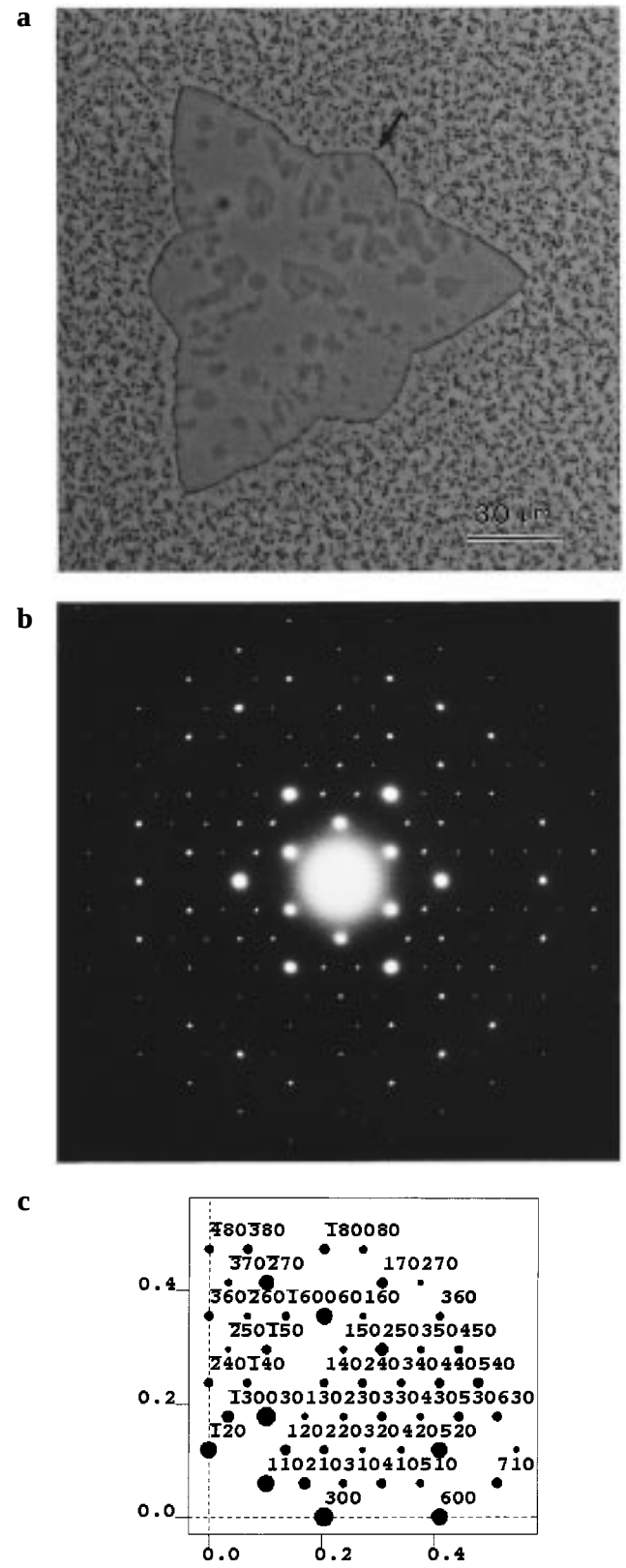

Figure 1. (a) Single crystal of PTBES grown in a thin film at 130 °C under a nitrogen atmosphere. Note the hump in the center of the growth faces, not observed under all crystallization conditions. Optical micrograph, phase contrast. (b) Electron diffraction pattern of a crystal as in part a in proper relative orientation. (c) Indexing of the pattern in part b generated with the Cerius[2] package on the basis of a three-chain trigonal unit cell of parameters $a = b = 16.91$ Å and $c = 6.50$ Å.

Epitaxially crystallized films of PTBES are produced using benzylpenicillin as a substrate. This compound is selected on account of the near-matching of a characteristic 9.36 Å periodicity (which was already used to induce the $(\bar{4}10)$ contact plane in monoclinic polyethylene)[6] and the interhelix distance (9.76 Å) in the densely populated (110) plane of PTBES. Crystals of benzylpenicillin are produced by precipitation on cooling of a chloroform solution and deposited with their mother liquor on the solvent-cast PTBES films. After evaporation of the mother liquor, the PTBES is melted at 180 °C (the benzylpenicillin is not affected by this treatment) and recrystallized for 2 h at 130 °C.

3. Experimental Techniques. The single crystals of PTBES and epitaxially crystallized films are observed in optical microscopy by phase contrast and by electron microscopy using a Philips CM12 microscope equipped with a rotation-tilt stage. Diffraction patterns are recorded on Kodak DEF 5 films and, in one set of experiments, on Fuji plates.

Molecular modeling was performed with the Cerius[2] program developed by Biosym-Molecular Simulations (Waltham, MA, and Cambridge, U.K.) run on a Silicon Graphics Indigo 2 workstation.

Results

1. Crystal Morphology and Diffraction Evidence. Single Crystals and *hk*0 Patterns. The single crystals produced by thin film growth have an unusual and characteristic *triangular shape* (Figure 1a). As indicated in a recent article,[7] this triangular shape is a common, but by no means systematic, characteristic of frustrated polymer crystal structures. More specifically, it indicates an intrinsic asymmetry of the crystal structure, in the sense that opposite sides of the growth planes have different structures, and therefore different growth rates.

The *hk*0 diffraction patterns obtained from single crystals as in Figure 1a display a trigonal or hexagonal symmetry (Figure 1b). The strongest ones can be indexed on the basis of a small, one-chain trigonal unit cell with parameters $a = b = 9.76$ Å, which corresponds to the subcell determined by Matsubayashi et al.[3] A number of weaker reflections indicate, however, a larger unit cell with an *a* parameter of 16.9 Å, of which the smaller cell is only a subcell (cf. indexing in Figure 1c). The availability of a full *hk*0 pattern makes it possible to recognize differences in intensity for *hk*0 and *kh*0 reflections, a feature that is not accessible to X-ray fiber patterns but would be anticipated for frustrated structures (cf. later). In the present case, however, it must be noted that *some* reflections (140, -150, 170, -180), which are symmetrically located relative to 0*k*0 ones (and $0\bar{6}0$ in particular), have different intensities for *hk*0 and $\bar{h}k0$, suggesting the impact of some dynamical scattering. This feature will be useful when analyzing the growth twins of PTBES.

The relative orientation of the diffraction pattern and crystal in Figure 1 indicates that the growth faces of the triangular crystals are of (100) type (and not {110}, as incorrectly indicated in ref 5): the growth planes do not therefore correspond to the most densely packed planes in the structure, in line with similar observations with crystals of frustrated polymer structures.[7] It should be noted, however, that for large crystals as shown in Figure 1a, and possibly as a result of depletion of crystallizable material, large scale crenellation of the growth faces develops, which leads to local orientations at 30° to the macroscopic growth front, i.e., to {110}

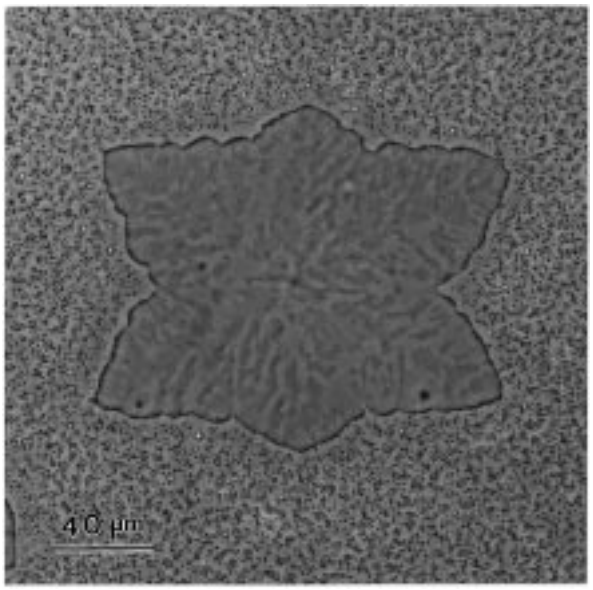

Figure 2. Twinned single crystal of PTBES grown in a thin film at 130 °C under a nitrogen atmosphere. Optical micrograph, phase contrast.

growth faces (cf. in particular the hump located in the middle of the growth faces, arrowed in Figure 1a).

A few twinned crystals have been observed (Figure 2). They correspond to the association of two "base parts" of the original triangles and are reminiscent of, but different in their details from, so-called "hourglass" associations of two triangular crystals of poly(β-benzyl L-aspartate) reported by Alegre et al.[8] Electron diffraction analysis of the twins makes use of the asymmetry of some $hk0$ and $\bar{h}\bar{k}0$ reflections indicated previously. It confirms that the pattern is symmetrically oriented with respect to the twin plane. Had this asymmetry not existed, the two components of the twin would have been indistinguishable on the basis of their $hk0$ diffraction pattern.

Epitaxial Crystallization and *hkl* Patterns. The epitaxially crystallized films (Figure 3a) yield further information on the PTBES crystal morphology and structure. In the films, lamellae are seen edge-on and are oriented in a single orientation relative to the substrate. Lamellar thicknesses determined by EM (Figure 3b) are in the 25 nm range. Electron diffraction patterns (Figure 3c, indexing in Figure 3d) indicate that the strong reflections on the equator are 300 (with the large cell), thus indicating that a densely populated plane of type {110} is the contact plane. The epitaxy therefore rests on the matching of the substrate 9.36 Å periodicity and the 9.76 Å PTBES interhelix distance. In Figure 3c, the zone axis of the epitaxially crystallized film is [100]. Rotation by 30° of the sample mounted on a rotation-tilt stage makes it possible to access the [110] zone axis (Figure 3e). Analysis of these diffraction patterns (1) confirms the 16.9 Å a axis periodicity, evidenced by the presence of all $h01$ reflections, (2) confirms the 6.5 Å chain axis repeat distance and the 3-fold symmetry of the helix, and (3) provides an interesting clue about the crystal structure. On the third layer line, it is apparent that the meriodional 003 reflection is *weaker* than its neighbor 103 ones. This feature was already noted by Turner-Jones et al.[9] when analyzing the X-ray powder pattern of isotactic polypropylene (iPP) in its β phase. Although these authors could not determine the exact crystal structure (which turns out to be a frustrated one),[4,10] this very characteristic allowed them to eliminate potential crystal structures, and notably structures based on a one-chain unit cell with standard $P3_1$ symmetry, for which 003 should be the strongest reflection on the third layer line.

2. Crystal Structure Derivation. The crystal structure derivation rests for a large part on the founding work of Matsubayashi et al.[3] It uses the 3-fold helix conformation derived by these authors but reassesses the packing of the helices in the unit cell. As already alluded to in the Introduction, it is indeed this packing that appears to be the weaker part of the structure derivation. The assumptions used for the initial structure derivation will be analyzed first and compared with the frustrated structure. The details of the structure are then given.

Nonfrustrated Structure of Matsubayashi et al. Figure 4a represents the structure of PTBES as derived by Matsubayashi et al.[3] It is based on a 3-fold helix conformation with a c axis repeat distance of 6.5 Å (calculated diffraction patterns in Figure 4c,d). The space group selected to account for the three-chain, trigonal unit cell is $P3_1$. As illustrated in Figure 4b, the crystallographic repeat unit is a single chain (marked A), which by virtue of the three 3-fold axes, generates the two other chains (marked B and C), and the smaller subcell has a symmetry close to $P3_121$.

The selection of the $P3_1$ space group in this specific use creates, however, significant problems. The argument rests on relatively straightforward considerations of crystal symmetry, as illustrated in schematic form in Figure 5 for a hypothetical helix, chosen here to be isotactic polypropylene. In Figure 5a, helices B and C, which are rotated by 120° in the ab plane, have nevertheless the *same azimuthal setting as helix A* (and indeed identical relative heights) on account of the 3-fold symmetry of the initial helix. In other words, the three-chain unit cell reduces to a smaller, one-chain subcell (cf. the expected fiber pattern, Figure 5b), in sharp contrast with diffraction evidence. To restore the larger cell, *an asymmetry should be introduced in the initial motif*. This is done in the model of Figure 5c by replacing a methyl group with a chlorine. The fiber pattern (Figures 5d) corresponds indeed to the larger three-chain unit cell.

In the structure of PTBES derived by Matsubayashi et al., the break of symmetry was achieved *by assuming different conformations of the side chains*, i.e., by assuming a set of three fixed and different τ_4 values ($C_\alpha-C$ (*tert*-butyl) torsion angles). This restores indeed a three-chain cell diffraction pattern (Figure 4c,d) but as already indicated in the Introduction, the postulation of different and fixed values of τ_4 appears as physically injustified, especially since the similar environments of the helices do not call for such departures from helical symmetry.

Derivation of the Crystal Structure of PTBES. The above weaknesses in the derivation of the PTBES structure can be neatly resolved by assuming a frustrated structure. Frustrated structures of crystalline polymers have been found for polymers with 3-fold helical symmetry, especially for chiral ones.[4,5] They are characterized by the fact that two helices maximize their interactions at the expense of a third one. As a result, the unit cell is "naturally" a trigonal, three-chain cell. Frustration is manifested by the fact that the three helices have different azimuthal settings. Two major packing schemes have been identified, which are shown

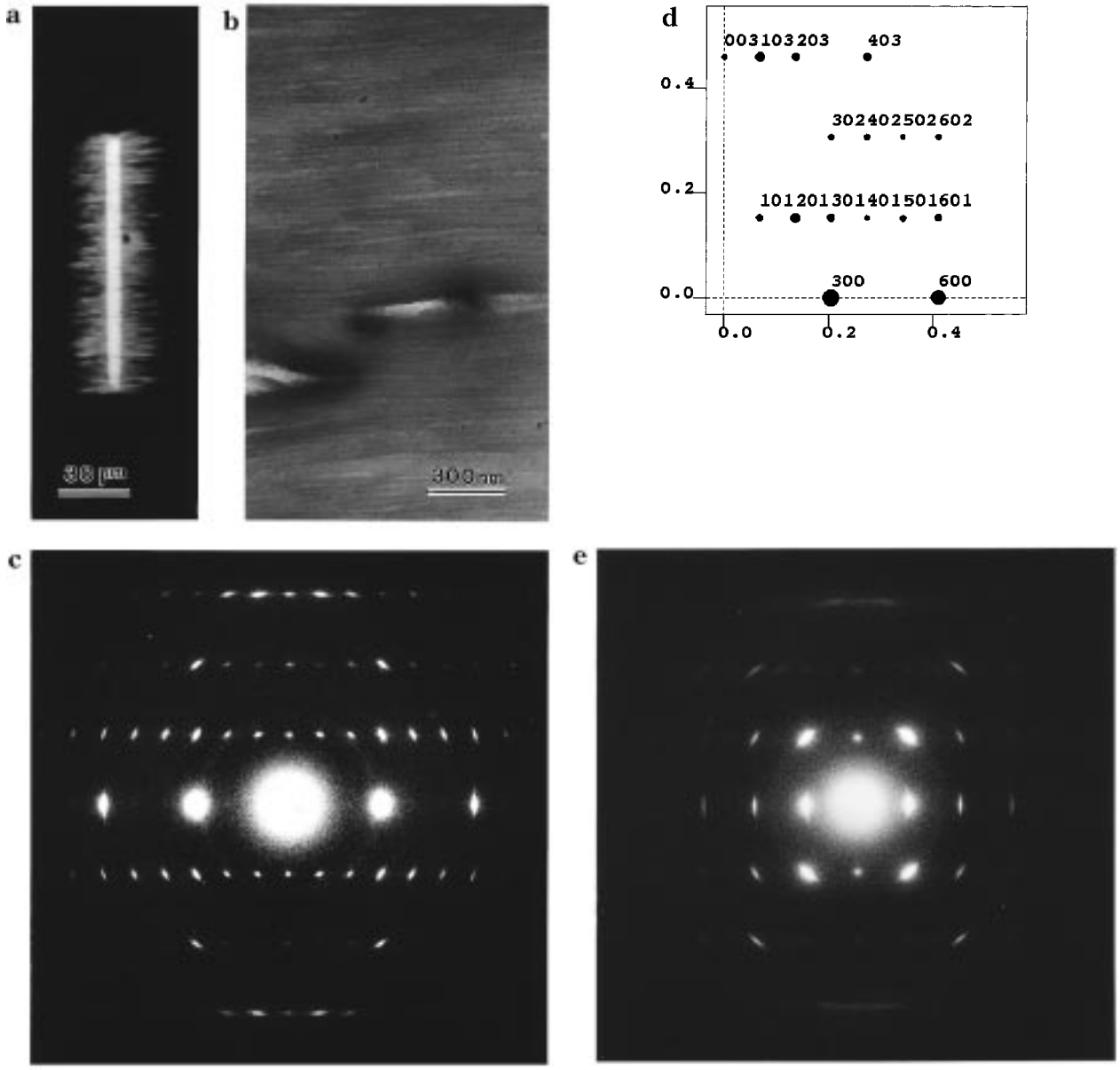

Figure 3. (a) Epitaxial growth of PTBES induced by a single crystal of benzylpenicillin. Note the rectangular shape of the substrate crystal and the extension of PTBES growth in the surrounding melt. Thin film growth at 130 °C. Optical micrograph, crossed polars. (b) Electron micrograph of part of a PTBES film as shown in part a after dissolution of the substrate. Note the lamellar organization (lamellar thickness: 25 nm) and the single orientation of the growth. (c) Electron diffraction pattern of part of the film shown in part b. Chain axis vertical. (d) Indexing of the pattern in part c. Zone axis: [010], indicating a (110) type contact plane. (e) Electron diffraction pattern of the film shown in (b) after a 30° rotation around the [001] axis.

schematically in Figure 6. They can be described by the set of orientations (on a compass) of one side chain of their three helices, i.e., as North−South−South (NSS) and North−East−East (NEE). Since analysis of the PTBES diffraction data leads us to prefer the latter packing scheme, we present first a general derivation of this model and develop next the details of the structure.

Derivation of the Frustrated NEE Packing of Helices. The derivation starts from a "standard" $P3_1$ packing scheme of 3-fold helices, as illustrated in Figure 7a, in which residue heights are expressed in sixths of the chain axis repeat distance *c*. If one considers the interactions of the side chain located at height 4 of the helix at the bottom of the figure (marked (a)) with those (0 and 2) of the facing helix (marked (b)), it becomes immediately apparent (Figure 7b, left) that these interactions cannot correspond to a minimum of the packing energy map: within the confines of the $P3_1$ space group, side chain 4a (shaded) is located on a "path" between two "hills" corresponding to the facing residues 0 and 2. A more satisfactory location of side chain 4a is obtained by shifting and moving it to a location (Figure 7b, right) in which it rests in a niche created by the "tripod" made of two residues at levels 0 (one *c* axis repeat apart) and one residue at level 2. This operation is at the root of a frustrated packing. Indeed:

—It privileges the interactions between two helices at the expense of a third one.

—Since relocation of residue 4 in position 3 involves a small rotation of the helix on its axis (and *c* axis shift), the azimuthal settings of the helices depart slightly from their initial one.

—The same interactions can be reproduced with other neighbor helices to helix b, but only according to a honeycomb lattice (indicated by the unshaded helices in Figure 7c); this specificity creates a "dual Kagome"

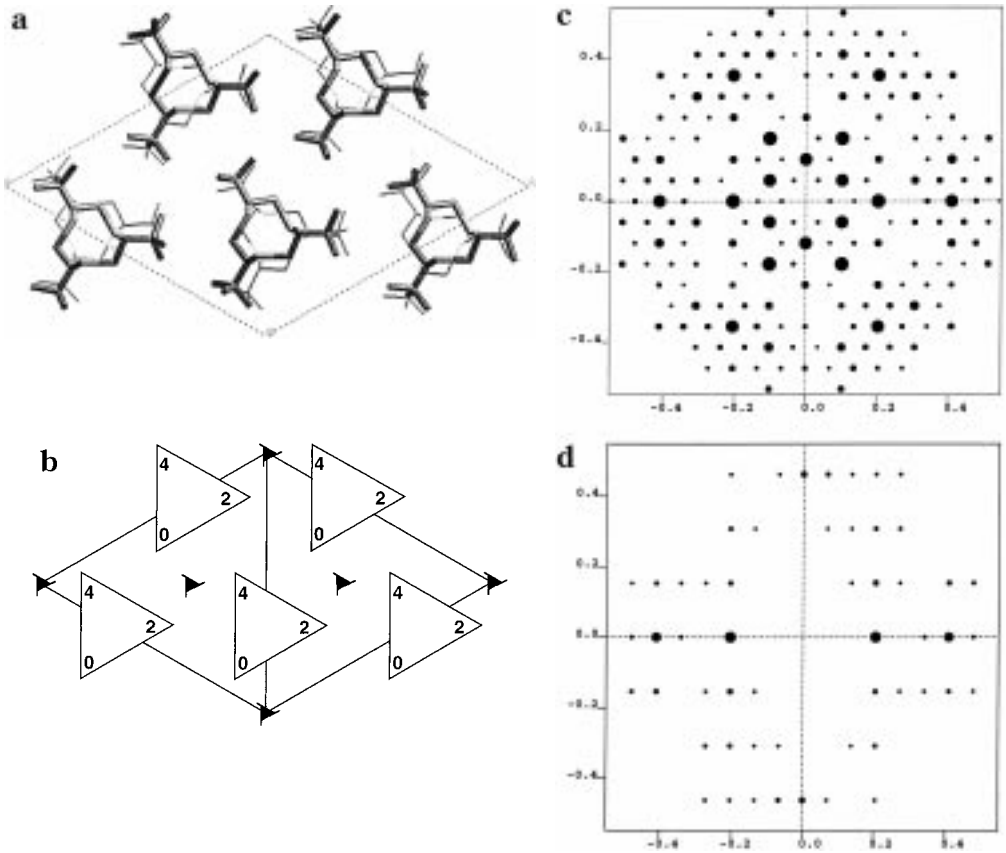

Figure 4. (a) Crystal structure determined for PTBES by Matsubayashi et al.[3] Note the identical azimuthal settings of the helices and the different settings of the side chain *tert*-butyl units. These settings are at the root of the three-chain unit cell. Up and down helices are shown as dark and light, respectively. (b) Symmetry elements of the structure shown in part a. (c) Calculated *hk*0 electron diffraction pattern of the structure shown in part a. Indexing as in Figure 1c. (d) Calculated *h*0*l* electron diffraction pattern of the structure shown in part a. Indexing as in Figure 3d.

or "diced lattice" scheme[11] (i.e., it generates a frustrated structure) (Figure 7c).

—Whereas the azimuthal settings of the two helices just considered are not significantly different from one another, the setting of the third helix is more affected. Indeed, this helix must find a satisfactory location within the helical "tube" generated by its six neighbors. *Its packing is less favorable than that of the other helices, thus the term of frustration.* A likely setting of the helix, the details of which need be determined by minimization of the overall packing energy, is represented in Figure 7c, which differs significantly from the azimuthal orientations of the two other helices. *Frustration of the packing is most clearly illustrated by this different azimuthal setting.*

—The new packing (Figure 7d) is best represented on the basis of the new, three-helix unit cell indicated. Curiously, *it rests on the same* $P3_1$ *space group* as the initial, one-helix unit cell. However, the helices are now centered on the 3-fold screw axes: the latter are therefore "used up" to generate the helices *from three different monomer units (one for each helix) rather than from a single 3-fold helix.* As a consequence also, the three helices are no longer linked by any symmetry operator. This feature is consistent with their different azimuthal settings and underlines the major difference with the derivation of Matsubayashi et al.[3] As a further consequence, and as in that work, up and down pointing helices are defined independently and similarly are not linked by any crystallographic operator. On steric and packing energy grounds, it is, however, reasonable to anticipate that substitution of an up by a down helix should be nearly isostructural and notably that the positions of the side chains should not be significantly affected. Up and down pointing helices are considered to be statistically present at each chain site.

—According to the model shown in Figure 7d, the locations of corresponding side chains of the center helices are at levels 3*c*/6 and 4*c* /6, i.e., are one-sixth of the *c* axis period apart. This feature implies that the relative *c* axis shifts of the three helices are nonuniform. In addition, the shifts of the two central helices are such that their contribution to the meridional 003 reflection cancels out, thus accounting for the characteristic weakness of this specific reflection of frustrated structures.

—It is worth emphasizing that the derivation of the frustrated structure shown in Figure 7d considers only the *location* of the side chains, irrespective of the main chain architecture. More specifically, it does not consider a possible *polarity* of the main chain (either chemical or conformational). It is therefore clear that the type of azimuthal frustration defined here can occur irrespective of chain "sense", i.e., *is not linked with parallelism or antiparallelism of helices*, as would be expected for chain-folded polymer single crystals. This point will be further analyzed in a later section.

Frustrated Structure of PTBES. The structure makes use of the low-energy chain conformation derived by Matsubayashi et al.[3] for PTBES. The structure derivation thus sums up in the differentiation of NEE from the alternative NSS packing mode, i.e., the determination of the azimuthal orientation of the three helices and their relative *c*-axis shifts. The analysis is

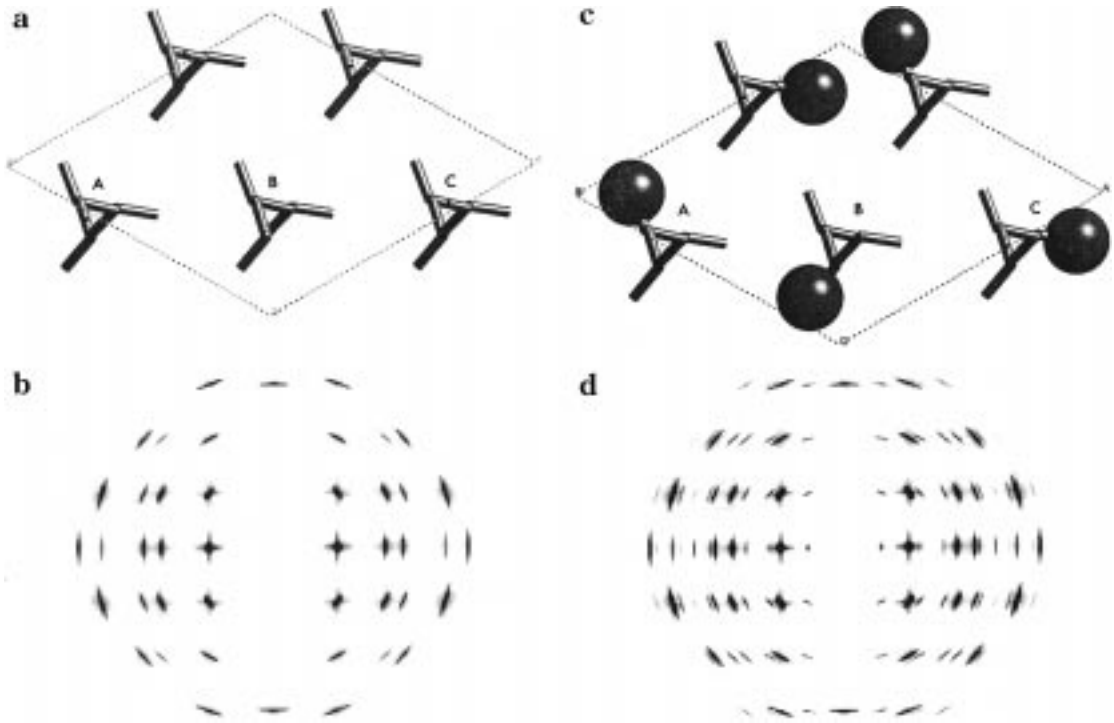

Figure 5. Illustration of diffraction patterns expected for various crystal structures (here of a polypropylene helix) based on the $P3_1$ space group, in the setting used in ref 3. (a) Generation of three 3-fold helices with identical setting angles and similar profiles from a repeat unit which is a full helix (marked A). (b) The fiber diffraction pattern corresponds to a smaller, one-chain subcell. (c) Breaking the 3-fold symmetry of the helix (here by replacing a methyl with a chlorine) restores the three-chain unit cell. (d) The fiber pattern corresponds to the three-chain cell.

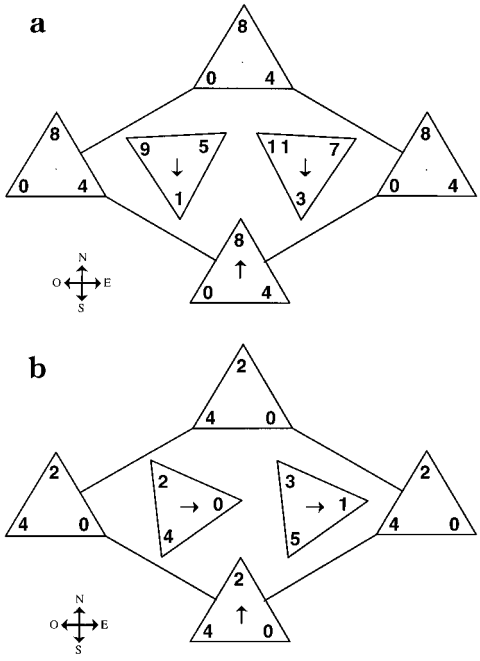

Figure 6. Two models of frustrated packings of 3-fold helices observed so far. The models differ by the azimuthal orientations of the helices in the cell, which are characterized by the orientation of the side chain closest to a cardinal point on a compass. Thus the sequence of orientations are (starting with the corner helix) NSS (a) and NEE (b). The heights of the side chains are expressed as mutiples of *c*/12 (a) and *c*/6 (b).

unambiguous: PTBES conforms to the NEE packing mode. Only this packing mode can account for the *relative* intensities of *all* observable reflections of the *hk*0 pattern up to reciprocal spacings of 0.5 Å^{-1}. The final structure is shown in Figure 8a, and its calculated *hk*0 and *h*0*l* diffraction patterns are displayed in Figure 8b,c (to be compared with the experimental patterns and the patterns predicted for the nonfrustrated structure of Figure 1b and 4c and 3c and 4d, respectively).

It should be noted that:

—The best agreement of calculated and observed patterns is obtained for a statistical unit cell with half occupancy of up and down chains at each site.

—The central helices are rotated counterclockwise by a standard, rather small 7° angle relative to the pure "East" orientation. This feature reflects the better location of the side group in the "niche" indicated in the derivation of the model.

—The corner helix is rotated by a full 15° from pure North orientation, but in the same counterclockwise sense as the central helix, which means that the *difference* in azimuthal setting with the two other helices is 22°.

—Up and down chains have near identical locations of the *tert*-butyl groups. However, and contrary to the model of Matsubayashi et al.,[3] the τ_4 torsion angle is not included, and actually required, as a variable in the structure derivation: the *tert*-butyl is essentially considered as an oversized methyl group. The τ_4 value has been fixed for the different side chains at 68°, which corresponds in *c* axis projection to the most "symmetrical" setting, and therefore deemphasizes its impact on the *hk*0 intensities. In addition, it corresponds to a satisfactory minimum of the helix energy.

—The model that yields the best agreement with electron diffraction data is also located in a comfortable minimum in terms of packing energy (−45 kcal/cell). This statement holds true irrespective of the up or down orientation at any helix site.

—The above criteria are very sensitive to small variations in the structural model and are therefore very compelling ones indeed, despite the qualitative approach used here. As an illustration, the various helices have

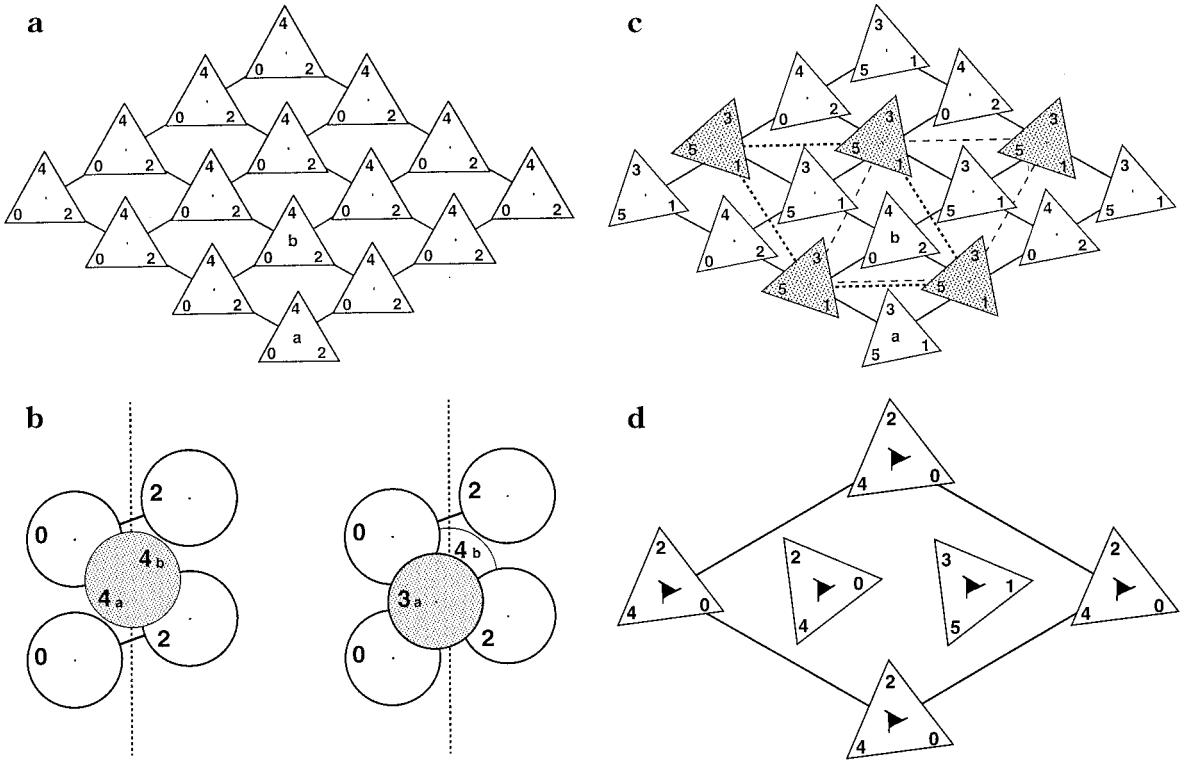

Figure 7. Derivation of the frustrated packing of 3-fold helices: (a) The one chain trigonal unit cell with "standard" orientation of 3-fold helices with relative side chain heights expressed in *c*/6 axis repeat distances. (b) (Left) Schematic illustration of the interactions between side chains of helices marked a and b in the lattice shown in part a, as observed from the bottom of that figure. The side chain at level 4 (shaded) of the front helix (a) interacts with side chains 2 and 0 of the underneath helix (b) and is located on a "path" between the 0 and 2 "hills". (Right) Possible location of side chain 4 of helix a (now at level 3) where it interacts with three neighbor side chains. (c) Structural consequences of the new location defined in part b. The two interacting helices become the central helices of a three-chain trigonal lattice. The interactions defined in part b can be repeated, but only on a honeycomb network of helices shown here unshaded. The central helix (shaded) cannot be involved in the same pattern of interactions. It adjusts its azimuthal setting and relative height in the "tube" created by its six neighbors. Note that the new structure can be described as North−East−East or South−West−West (cf. the two lattices with different dashed lines). (d) Resultant model of the frustrated structure shown in part c after a *c*/6 shift to conform to the pattern displayed in the models. Note that the new, three-chain cell has the symmetry elements of the $P3_1$ space group used in part a for the one-chain cell.

been rotated by a standard +5° on their axis. The packing energy increases only slightly, but calculated *hk*0 intensities display significant discrepancies with the single-crystal diffraction pattern. On this basis, the azimuthal setting of the helices is determined to better than a few degrees. (A more quantitative analysis of the data is under way, including assessment of dynamical scattering.)

The availability of a full set of *hkl* diffraction data obtained on epitaxially crystallized samples (cf. Figures 3c,e) makes it possible to confront the noneven *c* axis shifts of the three helices with experimental data. As already indicated, the most characteristic feature is the relative strength of 103 and 003 reflections illustrated in Figure 3c. An even *c* axis shift of the three helices would result in a 003 reflection more intense than 103 (Figure 4d). This is not the case and is fully accounted for by the frustrated structure.

Some minor discrepancies between observed and calculated *h*0*l* diffraction patterns do, however, exist. In particular, no 001 reflection is predicted, whereas this reflection shows up on the meridian of the first layer line. The reasons for its presence are unclear. It may reflect a break of exact 3-fold symmetry as assumed in our model (regarding, in particular, the constancy of τ_4 angles). However, similar features are observed in the *h*0*l* pattern of epitaxially crystallized iPP in its (frustrated) β form,[10] for which the side chains are methyl groups, and for which no impact of τ_4 is expected. On this basis, the presence of this reflection suggests rather some lattice disorder or streaking associated with thin film effects (for PTBES, an epitaxially crystallized film ≈10 nm in thickness corresponds to ≈12 layers only).

To conclude this derivation of the crystal structure of PTBES, we report in Tables 1 and 2 the atomic coordinates of the final structure arrived at, and the calculated structure factors, which complement the visual comparisons provided by Figure 1b and 8b for *hk*0 and 3c and 8c for *h*0*l* patterns.

3. Crystal Structure and Morphology of Single Crystals. As already detailed in a recent paper devoted to triangular single crystals,[7] the crystal structure based on a frustrated packing of helices accounts in a most natural way for the triangular morphology of PTBES single crystals. The triangular morphology can only be explained by different topographies of oppositely oriented (100) growth faces, which is a distinctive feature of this packing. Actually, the constancy of this triangular morphology provides also an interesting clue about the "constancy" of the frustrated scheme throughout crystal growth. In particular, *no growth twins are observed*, by which a "tip" would be nucleated on a "flat" face—a possibility that would be fully admissible on simple growth kinetics criteria. In other words also, the azimuthal setting of the chains remains constant: once an NEE pattern (for example) is established, it goes on unperturbed throughout the growth of the whole crystal. In particular, the pattern of helix orientations is not

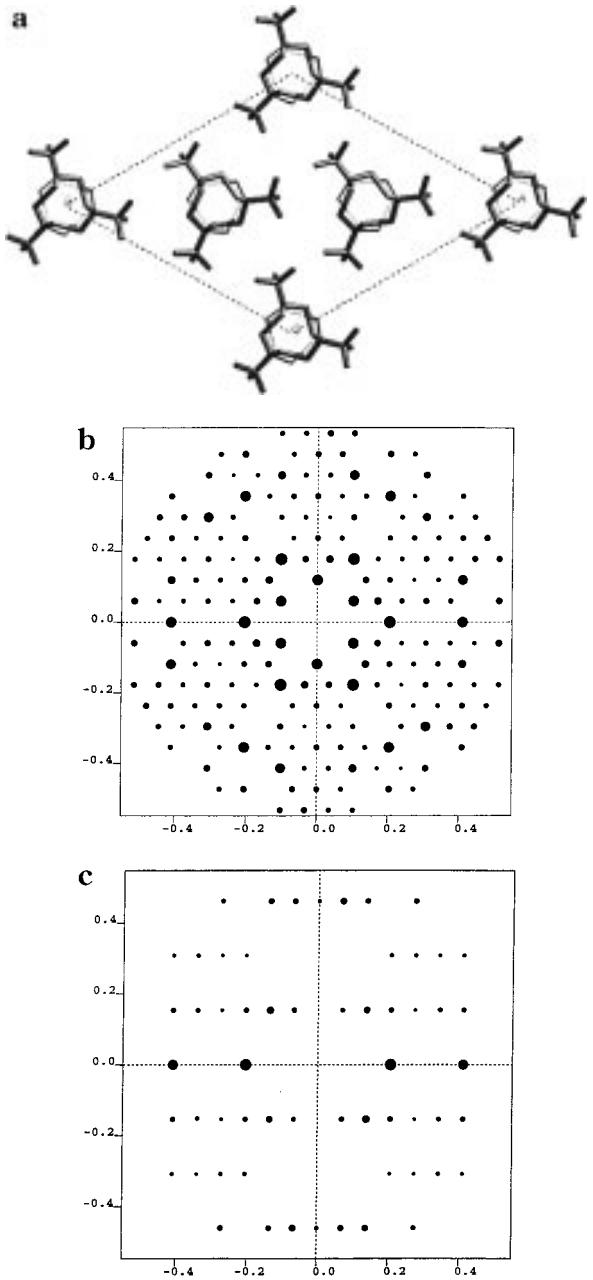

Figure 8. (a) Structure of PTBES as derived in the present work. Up and down chains are represented as dark and light, respectively. Note the different azimuthal setting of the corner chain relative to the center ones. The relative heights conform to the pattern indicated in Figure 7d. (b) Simulated *hk*0 electron diffraction pattern of the model shown in part a with the size of the dots proportional to the calculated intensity of the reflections (compare with Figure 1b). The differences in intensity for reflections affected by dynamical scattering are not reproduced. (c) Simulated 0*kl* electron diffraction pattern anticipated for the model shown in part (a) (compare with Figure 3c).

sensitive to (and therefore not induced by) parallelism or antiparallelism of the depositing helices. Even for a chemically "polar" polymer such as PTBES, the (near) isostructurality of up and down helices allows statistical substitution at each chain site, which in turn is fully compatible with chain folding as exists in single crystals. Note, however, that the issue of parallelism and antiparallelism of helices may become more involved, as analyzed by Puterman et al. for isotactic poly(4-vinylpyridine),[12] and as discussed in the companion paper for poly(L-hydroxyproline).[13]

Table 1. Atomic Coordinates of the Structure of PTBES[a]

	up				down		
atom	a	b	c	atom	a	b	c
S_A	0.4232	0.7373	0.5550	S_A	0.4279	0.7071	0.0231
$C_A(1)$	0.3496	0.7880	0.5490	$C_A(1)$	0.4162	0.7962	0.3631
$C_A(2)$	0.4632	0.7457	0.2920	$C_A(2)$	0.4635	0.7446	0.2861
$C_A(3)$	0.5676	0.8081	0.2840	$C_A(3)$	0.5676	0.8086	0.2941
$C_A(4)$	0.5950	0.8979	0.3971	$C_A(4)$	0.5934	0.8986	0.1836
$C_A(5)$	0.5996	0.8278	0.0591	$C_A(5)$	0.5994	0.8277	0.5192
$C_A(6)$	0.6138	0.7592	0.3916	$C_A(6)$	0.6154	0.7617	0.1845
S_B	0.7564	0.4042	0.3880	S_B	0.7607	0.3726	−0.1439
$C_B(1)$	0.6849	0.4551	0.3810	$C_B(1)$	0.7509	0.4628	0.1961
$C_B(2)$	0.7965	0.4100	0.1250	$C_B(2)$	0.7967	0.4097	0.1191
$C_B(3)$	0.9009	0.4718	0.1180	$C_B(3)$	0.9011	0.4723	0.1271
$C_B(4)$	0.9284	0.5630	0.2258	$C_B(4)$	0.9284	0.5627	0.0166
$C_B(5)$	0.9322	0.4906	−0.1076	$C_B(5)$	0.9329	0.4909	0.3521
$C_B(6)$	0.9474	0.4245	0.2249	$C_B(6)$	0.9474	0.4240	0.0175
S_C	0.0951	0.0452	0.3880	S_C	0.0859	0.0076	−0.1550
$C_C(1)$	0.0621	0.1313	0.3810	$C_C(1)$	0.1143	0.1141	0.1850
$C_C(2)$	0.1272	0.0359	0.1250	$C_C(2)$	0.1273	0.0356	0.1080
$C_C(3)$	0.2291	0.0650	0.1180	$C_C(3)$	0.2295	0.0656	0.1160
$C_C(4)$	0.2855	0.1579	0.2259	$C_C(4)$	0.2855	0.1576	0.0055
$C_C(5)$	0.2597	0.0741	−0.1076	$C_C(5)$	0.2605	0.0742	0.3410
$C_C(6)$	0.2449	−0.0072	0.2249	$C_C(6)$	0.2448	−0.0076	0.0064

[a] The atomic coordinates are given for one crystallographic repeat unit in each helix for up and down positions, assuming the space group $P3_1$. Unit cell parameters: $a = b = 16.91$ Å, $c = 6.50$ Å. Helices A and B: center left and center right, respectively. Helix C: corner.

Table 2. Calculated Structure Factors (F_c^2) and Observed Intensities (I_o) of PTBES[a]

	calculated				calculated		
hkl	*d* spacing (Å)	F_c^2	I_o[b]	*hkl*	*d* spacing (Å)	F_c^2	I_o[b]
110	8.455	35.03	vs	600	2.441	31.6	s
210	5.535	9.94	m	430	2.408	1.6	vw
300	4.882	51.68	vs	520	2.345	19.9	s
220	4.228	2.88	m	610	2.233	0.6	vw
310	4.062	2.4	w	440	2.114	1.3	vw
320	3.360	0.8	w	530	2.092	4.3	vw
410	3.196	4.1	s	620	2.031	0.4	vw
140	3.196	2.2	w	710	1.940	3.6	w
500	2.929	0.5	vw	170	1.940	7.4	m
330	2.818	3.8	w	540	1.875	4	vw
420	2.768	1.1	vw	630	1.845	1.1	vw
510	2.630	2.7	vw				

[a] The calculated structure factors are obtained from the simulated pattern of the frustrated packing with up and down chains as shown in Figure 7a. They are compared with the experimental intensities observed on the electron diffraction pattern of the triangular single crystal. [b] Key: vs, very strong; s, strong; m, medium; w, weak; vw, very weak.

Twinned crystals have been observed, but only when the initial nuclei are twinned, as attested by the fact that they are made of the association of two "bases" of individual crystals (Figure 2). A partial analysis of these twins is possible, based on the asymmetries of the diffraction pattern due to dynamical scattering. The problem sums up to establishing the orientation of the three helices in the unit cell in the two parts of the twin. The various orientations of a frustrated packing scheme are illustrated in Figure 9. They are, in short hand form and in *c* axis projection (i.e., again disregarding the up or down chain sense), NWW, NEE, SEE, and SWW. These orientations are linked by 2-fold axes parallel to *c* or *a* axes (inversion centers and planes of symmetry are excluded, since they would change the chirality of the polymer). Keeping in mind that the position of the strong reflections due to dynamical scattering changes on crossing the twin plane, it is clear that if one component of the twin is NEE, the second one is either NWW or SWW: there is no way to distinguish between these two possibilities, due to the special symmetry of the diffraction pattern (if the pattern had displayed true

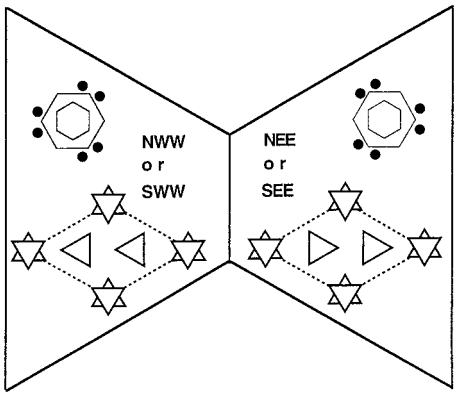

Figure 9. Illustration of the probable orientations of 3-fold helices of a frustrated structure relative to the edges of the triangular crystals and corresponding diffraction patterns in a twinned crystal. The growth faces of the crystals are of type (100). The positions of the reflections affected by dynamical scattering are shown in schematic form, the two inner hexagons representing the sets of 110 and 300 reflections. The two components of the twin can be distinguished by these reflections, which indicate that the central helices are oppositely oriented.

asymmetry with $hk0$ different from $\bar{h}\bar{k}0$, discrimination would have been possible).

The next step in the analysis is more speculative: it is reasonable to assume that the side of the (100) face growing fastest is that on which the helices deposit in a "notch" of the substrate face, i.e., when the helices have their tips oriented toward the face on which they deposit. Conversely, the slowest faces are those on which helices deposit with their base parallel to the substrate face (this step creates one extra lateral energy term).[7] On this basis, the orientation of helices indicated in Figure 9 is suggested as the most probable one. This analysis indicates that PTBES twins are π rotation twins with (100) twin planes, in which the central chains of the unit cell are in contact through their bases. It should be noted that the reverse situation could be envisaged, i.e., by permutating the NEE and NWW assignment. In that case, growth twins would be composed of two "tips" of triangles and have an overall lozenge shape, but the twin would be *formally strictly equivalent* to the previous one (same twin plane, same symmetry operator). While this possibility is not ruled out by growth kinetics, it has never been observed, suggesting that selection rules for growth twins of frustrated structures go beyond those of nonfrustrated ones.

Discussion and Conclusion

PTBES is only one among several chiral polymers that display an unusual crystal structure based on a *frustrated packing* of 3-fold helices, which had been neglected as a general packing scheme but for which various examples were established.[12,14] The present refinement of the structure initially proposed by Matsubayashi et al.[3] is therefore mainly concerned with establishing this frustration. It does not make full use of the diffraction evidence, available through both single crystals and epitaxially crystallized films; however, proper scaling of the relative intensities of all $hk0$ reflections of the electron diffraction pattern is a very compelling test indeed. Our analysis illustrates the improvements over available models of crystal structures, which can be achieved with the concept of frustration. It shows that frustrated structures *must* be described with the $P3_1$ space group (or $P3_2$, depending on helical sense) and definition of three *monomeric* crystallographic repeat units (six for up and down chains) that generate three (six) helices without any simple crystallographic relationship, apart from the constraints of near isostericity of up and down helices at each site.

The major change over previous structures is of course the introduction of different azimuthal settings of the helices at the three sites, which conform to a two-dimensional "diced" lattice or dual Kagome lattice, and which is at the root of the frustrated packing scheme. This change is quite dramatic, but once it is accepted, it avoids resorting to physically unrealistic assumptions, as have been made in the past for this[3] and for other[15] crystal structures. It also helps reanalyze the crystal structures of several polymers.[16,17]

PTBES also illustrates the relative constancy of the frustrated scheme throughout crystal growth: the "polarity" of the structure, indicated by one of the four sets of NEE, NWW, SEE, or SWW azimuthal orientations of helices, is defined at the level of the nucleus, and not modified during growth. Since the "polarity" of the structure shows up in the form of different surface topographies for opposite sides of the growth planes, a triangular single-crystal morphology emerges, which is a very unusual morphological indicator indeed:[7] it can be used as a valid experimental clue in the search of underlying frustrated crystal structures. This feature is used in the reevaluation of the structure of poly(L-hydroxyproline) in the companion paper.[13]

References and Notes

(1) Spassky, N.; Leborgne, A.; Sepulchre, M. *Croat. Chem. Acta* **1987**, *60* (1), 155.
(2) Dumas, Ph.; Spassky, N.; Sigwalt, P. *J. Polym. Sci., Polym. Chem. Ed.* **1974**, *12*, 1001.
(3) Matsubayashi, M.; Chatani, Y.; Tadokoro, H.; Dumas, P.; Spassky, N.; Sigwalt, P. *Macromolecules* **1977**, *10*, 996.
(4) Lotz, B.; Kopp, S.; Dorset, D. *C. R. Acad. Sci. Paris* **1994**, *319*, 187.
(5) Cartier, L.; Spassky, N.; Lotz, B. *C. R. Acad. Sci. Paris* **1996**, *322*, 429.
(6) Wittmann, J. C.; Lotz, B. *Prog. Polym. Sci.* **1990**, *15*, 909.
(7) Cartier, L.; Okihara, T.; Lotz, B. *Macromolecules* **1997**, *30*, 6313.
(8) Alegre, C.; Munoz-Guerra, S.; Subirana, J. A. *Macromolecules* **1989**, *22*, 3802.
(9) Turner-Jones, A.; Aizlewood, J. M.; Beckett, D. R. *Makromol. Chem.* **1964**, *75*, 134.
(10) Dorset, D.; McCourt, M.; Kopp, S.; Schumacher, M.; Okihara, T.; Lotz, B. *Polymer*, in press.
(11) Syozi, I. In *Phase Transitions and Critical Phenomena*; Domb, C., Green, M. S., Eds.; Academic Press: London, New York, 1972; Vol. 7, p 269.
(12) Puterman, M.; Kolpak, F. J.; Blackwell, J.; Lando, J. B. *J. Polym. Sci., Polym. Phys.* **1979**, *15*, 805.
(13) Cartier, L.; Lotz, B. *Macromolecules* **1998**, *31*, 3049.
(14) Meille, S. V.; Ferro, D. R.; Brückner, S.; Lovinger, A. J.; Padden, F. J. *Macromolecules* **1994**, *27*, 2615.
(15) Sasisekharan, V. *Acta Crystallogr.* **1959**, *12*, 903.
(16) Cartier, L. Thesis, Université Louis Pasteur, Strasbourg, 1997.
(17) Lotz, B. *Polym. Prepr. (Am. Chem. Soc., Div. Polym. Chem.)* **1996**, *37* (2), 430.

MA971844E